Temporal and spatial variability of hydrographic conditions along the innershelf of the Ross Sea obtained using instrumented seals

Andrea Piñones[1,2*], Eileen E. Hofmann[1], Daniel P. Costa[3], Kimberly Goetz[3], Jennifer M. Burns[4], Fabien Roquet[5], Michael S. Dinniman[1], John M. Klinck[1]

[1]Center for Coastal Physical Oceanography, Old Dominion University, Virginia, USA

[2]Centro de Estudios Avanzados en Zonas Áridas (CEAZA), Facultad de Ciencias del Mar, Universidad Católica del Norte, Coquimbo, Chile

Avenida Ossandón 877, Coquimbo, Chile

[3]Department of Ecology and Evolutionary Biology, University of California, Santa Cruz, USA

[4]Department of Biological Sciences, University of Alaska, Anchorage, USA

[5] LOCEAN/Museum National d'Histoire Naturelle, Paris, France

*Corresponding author: andrea.pinones@yale.edu

Tel: 56 (51) 2673259

Draft date: 31 January 2016

Submission to: *Journal of Marine Systems*

Keywords: Ross Sea, seal satellite tags, wind variability, density gradients, heat content

Abstract

Temperature and salinity measurements obtained from sensors deployed on Weddell seals (*Leptonychotes weddellii*) between February and November 2010, January to October 2011 and February to November 2012 were used to describe the temporal and spatial variability of hydrographic conditions in the western Ross Sea, with particular emphasis on the innershelf off Victoria Land and south of Ross Island. Potential temperature-salinity diagrams constructed for regions where the seals remained for extended periods of time showed four dominant water masses on the shelf, Modified Circumpolar Deep Water, Antarctic Surface Water, Shelf Water and Modified Shelf Water. Depth-time distributions of potential density and buoyancy frequency showed the erosion of the upper water column stratification associated with the transition from summer to fall/winter conditions. The within-year and interannual variability associated with this transition was related to wind speed and atmospheric temperature and pressure. Changes in upper water column density were positively correlated with cross-shelf wind speeds >5 m s^{-1} with a 3-4 day lag. A comparison of wind mixing potential versus stratification (Wedderburn number) showed that synoptic scale wind events with speeds of 5.5 and 6.5 m s^{-1} are required to erode the summer stratification for Ross Island and Victoria Land regions, respectively. The interannual variability in total heat content accumulated during summer (about 20%) was related to the duration open water, with the largest heat content occurring in 2012 which was characterized by a summer sea ice minimum. The heat content was lost by early to mid-March and approached zero in winter as a result of deep winter convection. The seal-derived measurements provide a

quantitative analysis of hydrographic variability of the innershelf region of the western Ross Sea and provide a baseline for assessing future changes.

Introduction

The advent of small electronic tags and their associated sensors that can be placed on a variety of marine animals has not only resulted in an amazing increase in our understanding of their movement patterns (Bost et al. 2009, Costa et al. 2012, Bost et al. 2015) but has also provided invaluable insights into the physical oceanography of the regions that are otherwise difficult or even impossible to sample (Charrassin et al. 2008, Roquet et al. 2009, Fedak 2013, Roquet et al. 2013). These small electronic tags are providing oceanographic data in areas where traditional shipboard and Argo-float coverage is limited or absent, particularly in the Southern Ocean where ship time is limited (especially in the winter), the capability of satellite remote-sensing systems is often reduced due to cloud cover, and as Argo floats are unable to work in ice and have a propensity to be advected away from the Antarctic Continent. To date sensors mounted on marine animals have helped to refine the bathymetry of the Antarctic Peninsula (Padman et al. 2010), to quantify the heat flux of oceanic currents and their importance in ice formation (Nicholls et al. 2008), facilitate the understanding of the breakup of ice sheets (Padman et al. 2012), better understanding of the basic hydrographic properties of Antarctic continental shelf systems, such as the seasonal progression of the thermohaline structure and heat content variability of the upper ocean mixed layer, more accurately identify frontal systems (Meredith et al. 2011, Årthun et al. 2012) and the general hydrography and circulation patterns of the Southern Ocean (Roquet et al. 2013).

Here we report the physical oceanographic observations from CTD tags deployed on Weddell seals (*Leptonychotes weddelli*) in the Ross Sea. Weddell seals are the southernmost seal and inhabit in the fast and pack ice regions, which are particularly difficult to access using any other methodology. The Ross Sea (Fig. 1) overlies the largest continental shelf in the Southern Ocean and is one of a few locations that forms and exports Antarctic Bottom Water (Orsi et al. 1999; Gordon et al. 2009; Budillon et al. 2011). The Ross Sea is experiencing increased sea ice (Comiso et al. 2011), decreased duration of the summer ice-free period (Parkinson 2002; Stammerjohn et al. 2008, 2011), decreased sea surface temperature (Comiso 2010), and stronger southerly winds (Turner et al. 2009; Holland and Kwok 2012); all of which affect the upper ocean thermohaline properties. However, projections for future trends are for reduced sea ice cover and longer ice-free periods (Smith et al. 2014b) and increased air temperature (Bracegirdle and Stephenson 2012). Much of the understanding of water masses, thermohaline properties, and hydrographic variability of the Ross Sea is derived from summer measurements during ice-free conditions. The changes in the upper ocean thermohaline properties in winter, which potentially set up conditions that influence subsequent sea ice cover and water mass formation, are little known and poorly resolved in hydrographic measurements from the Ross Sea.

As part of a study of predator winter foraging behavior and habitat utilization in the Ross Sea, conductivity-temperature-depth satellite relay data loggers (CTD-SRDL) were deployed on Weddell seals (*Leptonychotes weddellii*) over a three-year period (2010-2012) (Goetz, 2015). The seal-collected data provide extensive coverage of the southwestern Ross Sea (Fig. 1) from the austral summer, when the tags were deployed, through the winter and into the following austral fall. The consistent sampling region and multiple vertical profiles (seal dives) at many locations allow the seasonal evolution of the upper ocean variability to be characterized and compared over three years. The objectives of this study are to use the seal-collected temperature and salinity data to describe seasonal and interannual changes in the thermohaline properties and heat content of the upper ocean of the Ross Sea and relate these changes to wind, atmospheric temperature and pressure variability. This analysis provides a baseline for measuring future responses of the Ross Sea to projected changes in atmospheric forcing.

Methods

Seal tags. CTD Satellite Relay Data Loggers were deployed on Weddell seals from February to November 2010, January to October 2011, and February to November 2012 (Table 1). The accuracy for conductivity, temperature and pressure (depth) sensors is ± 0.003 mS cm^{-1}, ± 0.001°C, and ± 5 dBar, respectively. The tag is optimized to collect oceanographic data relative to the seal's descent and ascent speeds (~1 m s^{-1}). Data collected by the tag are stored and transmitted to the ARGOS satellite system when the animal is at the surface. . The CTD profiles are summarized prior to ARGOS transmission by four inflection points that correspond to the most rapid changes in the time-depth trajectory (i.e. local maxima of the second derivative of the time-depth function). Data are collected at 2 Hz and summarized into 20 points including 10 fixed pressures adaptively selected based on the maximum pressure of the dive, and augmented by 10 points selected by a broken-stick algorithm (Rual 1996; Fedak et al. 2001; Fedak et al. 2002). ARGOS cannot transmit all records so a pseudo-random method is used to transmit an unbiased sample of stored records. The tags were calibrated prior to deployment and comply with ITS-90 (International Temperature Scale 1990) and PSS-78

(Practical Salinity Scale 1978) specifications. Additional details of seal tagging procedures are provided in Burns et al. (2004) and Gales et al. (2005).

Temperature and salinity data. The tagged seals moved throughout the western region of the Ross Sea (Fig. 1b-d) and information on quality control of the tag data and analyses of the distributional data are given in Roquet et al. (2011) and Goetz (2015). More than 79% of seal dives that returned temperature and salinity data were from the innershelf off Victoria Land, around Ross Island, and in 2010 along the outer shelf (Fig. 1b-d). The data from Victoria Land and around Ross Island provide the basis for this study because these regions were consistently sampled in all three years. Following the approach used in Costa et al. (2008), the areas where the dive data were concentrated were binned into a 10 km x 10 km grid and the number of dives in each grid cell was counted (Fig. 1b-d).

The temperature and salinity measurements in each region were binned at 10-m and 1-day intervals and an average calculated for each bin. The temperature and salinity records from the seals provided coverage of the upper 300 m (Fig. 1b-d). The resulting data set for each region was used to construct potential temperature-salinity diagrams for all three areas (Fig. 2) and time-depth distributions for Victoria Land and Ross Island for 2010, 2011 and 2102 (Figs. 3, 4). For the latter, gaps of 3 days or less in the seal dive data were interpolated linearly.

The potential temperature and salinity distributions were used to construct time-depth distributions of density and buoyancy frequency to represent the vertical structure and stratification of the water column for each region in each year. Buoyancy frequency was calculated from:

$$N^2 = -g\partial\rho/\partial z \qquad (1)$$

where g is gravity (9.8 m^2 s^{-1}) and $\partial\rho/\partial z$ is the change in density (ρ) with depth (z).

Atmospheric data and sea ice fraction. Winds, atmospheric pressure and atmospheric temperature for the Ross Sea region for 2010 to 2012 were obtained from the ERA-Interim reanalysis (Dee et al., 2011) dataset. Values were extracted from the two grid points closest to Victoria Land and Ross Island at 6-hour intervals and used to calculated daily averages. The wind values were rotated to their major axis of variability, which corresponded to the across-shore direction. After rotation, the main axis of variability corresponded to winds blowing from land out over the ocean and the minor variability axis corresponded to winds blowing along the shore.

Sea ice distributions were obtained from simulations done using a high-resolution coupled sea ice – ice shelf – ocean circulation model implemented for the Ross Sea (Dinniman et al., 2011; Stern et al., 2013). Sea ice distribution and fraction was simulated for 15 September 2010 to 15 March 2012. For this study, daily-averaged sea ice fraction, the area covered by sea ice relative to the total area, was calculated for the Ross Island and Victoria Land regions using simulated distributions for December 2010 to November 2011 and November 2011 to December 2012. . These distributions represent the transition from late spring to winter. Modeled sea ice concentration closely represents observed sea ice concentration during the study period, for further information please see supplementary information in McGuillicuddy et al. (this issue)

Analysis methods. Cross-correlations and coherence and phase spectra (Emery and Thomson, 1998) were used to determine the relationship between atmospheric variables and water column vertical structure. Cross-correlations were estimated between the daily-averaged across-shore wind component, atmospheric pressure and atmospheric temperature and water column density (from surface to 300 m), Coherence spectra between across-shore wind and water column density were estimated for the Ross Island and Victoria Land regions using 8 and 10 degrees of freedom, respectively. Phase (days) was obtained for coherences above the significance level of 90%.

The interaction of wind events with summer stratification was explored using a Wedderburn number (*W*), which provides a measure of mixed layer stability (*W*>1) or instability (*W*<1) based on the balance between wind forcing and the pycnocline tilt (Imberger, 1985), and is calculated as:

$$W = (g'\,h^2)/(u_*^2 L) \tag{2}$$

where $g' = g\Delta\rho/\rho$ is the reduced gravity due to a density gradient $\Delta\rho$, h is depth of the summer mixed layer, $u_* = \sqrt{\tau/\rho}$ is the surface shear velocity due to wind stress (τ) and L is the length of the innershelf area in the direction of the wind (L=40km). Wind stress was estimated from wind records using a drag coefficient of 1.3×10^{-3} and air density of 1.2 kg m^{-3}. The seasonal mixed layer depth (*h*) was estimated using a density threshold defined by the shallowest depth at which the vertical density differed from the value at 15 m by 0.01 kg m^{-3} (Smith et al., 2011; Kaufman et al., 2014).

Heat content estimates. The total heat content (*HC*) of the upper 300 m (*zp*) was estimated from the time-depth distributions of potential temperature (T_p). The heat content was calculated relative to the surface freezing temperature (T_f= -1.9°C) at a salinity of 34.5 and surface pressure (0 dbar) as:

$$HC = \int_0^{zp} \rho c_p (T_p - T_f)\ dz \qquad (3)$$

where ρ is density of seawater and c_p is the specific heat of seawater (3994.6 J °C^{-1} kg^{-1}).

Results

Temperature-salinity patterns. Potential temperature-salinity (TS) diagrams constructed for the Victoria Land and Ross Island regions showed low interannual variability during summer (Fig. 2a, b, c). During the summer, the seals provided only a few observations from the mid-outer shelf. The TS diagrams show primarily Antarctic Surface Water (AASW) in the upper water column, characterized by low salinities (~34) and cold temperatures (-0.5 °C to -1.6°C). Fresh surface waters (33-33.8) were observed all three years in the Victoria Land region and only during 2012 for the Ross Island region. Modified Circumpolar Deep Water (mCDW, >34.4, -1.5-0.5 °C) lies below AASW and above modified shelf water (MSW, >34.5, > -1.85 °C).

The same three water masses are present in all three regions during fall-winter (Fig. 2d, e, f). Surface waters tend to remain fresher (<34) in the Victoria Land region in all three years. The AASW in the Ross Island region is colder than that in the Victoria Land region in all three years. Both regions show colder AASW during 2011. The mid-outer shelf is mostly occupied by mCDW. This water mass was well defined during 2010 and 2011 (Fig. 2d, e). The signal of this water mass is not as well defined in 2012 (Fig. 2f) because of the fewer number of CTD from the mid to outer shelf (Fig. 1). The winter

TS distributions show MSW and Shelf Water (SW, >34.5, <-1.85 ^{o}C) in all years at the three locations (Fig. 2d, e, f).

Water column characteristics. The depth-time distributions of density constructed for the Ross Island (Fig. 3a, b, c) and Victoria Land (Fig. 4a, b, c) regions in each year show the presence of less dense water at the surface in summer, as expected, and the erosion of this layer into fall. However the pattern of density progression varies between the two regions. The vertical density gradient in the Ross Island region persists until end of February during 2010 and 2011, and until mid-March during 2012. The vertical density gradient in the Victoria Land region is largely eroded by late February in 2010 and 2011, and persists until mid-March in 2012. The vertical density gradient at Ross Island is eroded by mid March during 2010 and 2012, and until late February in 2011. The vertical density gradient was stronger in Victoria Land (Fig. 4a, b, c), as a result of a shallow and fresh surface mixed layer depth that extended to 25 m. The pycnocline was deeper during 2010 and 2011 (~60 m) and shallower during 2012 (~40 m), stronger vertical gradients were observed for 2011 and 2102.

The time-depth evolution of the vertical density gradient in the two regions is reflected in the buoyancy frequency distributions (Figs. 3, 4d, e, f). Buoyancy frequencies of the order of 10^{-4} s^{-2} were frequent during 2012 in Ross Island and observed in the upper 50 m consistently until end of February. Buoyancy frequencies of the same order of magnitude were observed for only a few days during 2010 and 2011. In the Victoria Land region buoyancy frequencies of 10^{-4} s^{-2} were observed during 2011 and 2012 in the upper 50 m and only 2-3 days during 2010. The buoyancy frequencies calculated for the Victoria Land region were overall higher than those for the Ross Island region. This strong stratification disappeared in early March 2011 but remained until mid-March in 2012 (Fig. 4f).

Relationship with atmospheric conditions. The temporal variability of the upper water column can be related to wind events in both regions (Figs. 3, 4g, h, i). Across-shore wind (U-component) pulses are associated with deepening of the isopycnals below 50 m, which mixes low-density surface waters deeper in the water column. This response was observed for the Ross Island region for wind events with speeds that exceeded 5 m s^{-1} in all years (Fig. 3g, h, i). Similarly, strong wind pulses were associated with mixing downwards the low-density surface waters in the Victoria Land region (Fig. 4g, h, i).

The relationship between wind events and the erosion of summer stratification was investigated further by calculating cross-correlations between across-shore wind and density at depth for the Ross Island (Fig. 5a, b, c) and Victoria Land (Fig. 6a, b, c) regions in the three years. Significant positive correlations were obtained in the upper 150 m for the Ross Island region, with the onshore wind pulse leading by 3-4 days an increase in surface density (Fig. 5a-c). During 2010 and 2011 the increase in onshore wind was followed by a decrease of subsurface density 10 days later. This pattern was present during 2012 but correlations were not significant at the 95% confidence (Fig. 5c).

Atmospheric pressure and density were negatively correlated above 100 m for most of 2010 and 2011, and positively correlated during 2012 (Fig. 5d, e, f). The correlations change sign with depth. The vertical pattern in the pressure-density correlations is similar to that obtained for the wind-density correlations, with both showing a change in sign of the lagged correlations at depth (Fig. 5e-f). The same pattern was also observed between atmospheric temperature and density, with a decrease in temperature correlated with a surface increase in density and a subsurface decrease, and vice versa for increased atmospheric temperature (Fig. 5g-i).

In the Victoria Land region, similar wind-density correlation patterns were obtained, with the strongest correlations occurring in 2011 (Fig. 6a, b, c). Onshore wind pulses were correlated with density decreases in the upper 100 m. This effect was strongest in 2011, with significant correlations with a 3-4 day lag were found at all depths (Fig. 6d-f). In 2011, atmospheric pressure and density were positively correlated throughout the water column and significant positive correlations were observed between air temperature and density on the upper 200 m (Fig. 6e).

Coherence and phase spectra provide comparisons of the variability in across-shore wind and water density at different depths in the two regions in the three years (Figs. 7, 8). The Ross Island region showed significant coherences between onshore wind and density distribution below ~50 m at a 10-day frequency during 2010 (Fig. 7a) and below 100 m during 2011 and 2012 (Fig. 7c, e). Wind variability leads density variability by 2-5 days (Fig. 7b, d, f). Significant coherences were also observed at higher frequencies (~0.3 cpd, 3.3 days), during 2010 and 2012. Wind and density variability at 2-4 days was significant at about 55-155 m. In 2010 significant coherences were found within the synoptic weather band (5-10 days) between the onshore wind and density at mid-water level (55-155 m) in the Victoria Land region (Fig. 8). Wind variability leads density variability by 0-1 days (Fig. 8b). In 2011, significant coherences were observed at about 95-155 m in the lower frequencies (~0.1 cpd, 10 days). Wind variability at this temporal scale was followed by density variability with an 8-9 day delay. Significant coherences were also observed at higher frequencies (~3 days) between wind and density at depth (>95 m) with a 2-day delay (Fig. 8c, d). In 2012, significant coherences were observed only in the high frequencies and below 100 m (Fig.7e). The positive phases indicate that density variability leads the wind variability by 0-1 day (Fig. 8f).

The Wedderburn number provides a measure of the interaction of wind events, with scales of 5-10 days, with the summer stratification for the two regions (Fig. 9). Winds in excess of 8.9 m s^{-1} and 10.8 m s^{-1} are required to mix across the pycnocline and erode the summer stratification observed for the Ross Island (Fig. 9a) and Victoria Land (Fig. 9b) regions, respectively, in 2010 and 2011. Stratification was stronger in the Victoria Land region ($\Delta\rho$ = 1.5 kg m^{-3}) relative to the Ross Island region ($\Delta\rho$ = 1.1 kg m^{-3}), therefore requiring stronger winds to mix the water column. The estimated mixed layer depth was shallower in 2012 in both regions, and the wind required to erode the summer stratification was 5.5 and 6.5 m s^{-1} for Ross Island and Victoria Land, respectively (Fig. 9).

Heat content estimates. Heat content of the upper 300 m for the three years shows that the Ross Island region reaches maximum heat content earlier than Victoria Land (Fig. 10a,b). The minimum simulated fraction of sea ice between Ross Island and Victoria Land is consistent with the heat content patterns (Fig. 10c). The Ross Island region is essentially open water during the summer which allows the heat content to increase earlier than in the Victoria Land region where ice cover persists into the summer. The two regions showed small (<20%) interannual difference in the total heat content. The averaged heat content in both regions was lower (28% in Ross Island and 16% in Victoria Land) in 2011 and heat loss occurred earlier in the season. The largest accumulated heat content occurred in 2012, with heat accumulation persisting later into the summer and heat loss occurring later in the fall.

Discussion

Temperature-salinity characteristics. The seals provided autonomous oceanographic platforms that sampled the hydrographic variability of the western Ross Sea in locations and during times that are not accessible using conventional oceanographic sampling methods. The TS diagrams constructed from the seal data provide a characterization of the hydrographic properties of the Victoria Land and Ross Sea regions, which is dominated by the presence of AASW, SW, and MSW. The summer surface heating produces AASW that occupies most of the upper water column. The seasonal variability of this water mass is as expected in both regions. Sea ice formation during the fall and winter converts the nearly freezing AASW to SW (Orsi and Wiederwohl, 2009) and the layer of AASW is eroded. The air-sea interaction contributes to the interannual variability of the AASW water mass (Locarnini, 1994).

The water mass properties of the Ross Island and Victoria Land regions are also potentially influenced by inputs from other regions, Stern et al. (2013) showed that a warm signature observed in McMurdo Sound originated west of the Ross Sea polynya, and was produced by solar heating after the polynya is ice free. This warmer, fresher and therefore less dense surface water flowed west along the innershelf of the western Ross

Sea Ice Shelf creating a coastal current that flows along the north side of Ross Island and into McMurdo Sound.

Over the mid-outer shelf the signature of mCDW is similar in the three years. This water mass intrudes onto the Ross Sea continental shelf below 200 m at preferred sites (Dinniman et al., 2003; Stern et al., 2013). Thus, any interannual variability of this water mass is imposed by processes related to flow along the outer Ross Sea shelf (Dinniman et al., 2011). The mCDW mixes with the near freezing SW to produce MSW (Orsi and Wiederwohl, 2009). The latter water mass is found in the Victoria Land and Ross Sea regions in fall and winter. This provides a linkage between inputs of mCDW and the innershelf of the Ross Sea. The mCDW also provides heat to the shelf waters and underneath the Ross Sea Ice Shelf, with the latter contributing to the basal melt rate (Dinniman et al., 2011; Kohut et al., 2013; Stern et al., 2013).

Atmospheric forcing and stratification. The seal-derived observations suggest that summer stratification along the innershelf in the Ross Sea is primarily controlled by changes in salinity, which in turn controls density of the upper water column. Cross-correlations between atmospheric parameters and ocean density showed that onshore wind events with speeds in excess of 6 m s^{-1} are needed to induce vertical mixing that is sufficient to erode the summer stratification and allow mixing across the pycnocline. The correlations between onshore winds and increased surface density were significant in in both areas in the three years. Surface winds in the inner portion of the Ross Sea result from katabatic and synoptic wind events (Murphy and Simmonds 1993; Parish and Cassano, 2001; Parish and Cassano, 2003). Katabatic winds, with speeds of 10-25 m s^{-1}, occur in the Victoria Land and Ross Island regions (Parish and Bromwich, 1991;

Colacino et al., 2000; Parish and Cassano, 2003), with a main wind direction axis that is across the coastline (Colacino et al., 2000). The coastal regions of the western Ross Sea also experience frequent cyclone activity that also influences surface winds (Cassano and Parish, 2000). These synoptic scale events occur with a frequency of 3 to 10 days and are characterized by wind speeds of 15-35 m s^{-1} (Bromwich, 1991; Parish and Cassano, 2003).

Each wind event produces mixing in the upper ocean (< 200 m) that incrementally erodes the surface summer stratification, which is dominated by a low-density shallow surface mixed layer above a sharp pycnocline. The resulting entrainment of high-density water in the surface layer is seen in the summer-fall-winter progression of the upper ocean that is provided by the seal observations. The interannual variability in the erosion of the seasonal stratification seen in the time-depth density distribution can be related to the frequency and strength of the wind events. The more stratified innershelf during 2012 is consistent with less intense wind events (~<5 ms^{-1}); strong (>6-10 ms-1) wind pulses destratified the water column earlier during 2010 and 2011. The implication is that erosion of the seasonal stratification is an incremental process that is moderated by the frequency of wind events with speeds above a particular threshold.

Comparisons between atmospheric pressure, atmospheric temperature and ocean density yield significant correlations, further supporting those obtained with wind speed. The significant correlation with low atmospheric pressure at sea level is related to the pressure gradient difference responsible in the formation of katabatic winds (high pressure over the land plateau and low pressure over the sea). Decreased atmospheric pressure was correlated with an increase in surface density and a decrease in density at depth, as expected for mixing. Decreased atmospheric temperature was also correlated with increase of surface density. This correlation is, however, the result of the seasonal change in atmospheric temperature rather than the result of surface cooling due to katabatic winds. Atmospheric temperature is not a reliable measure of katabatic wind variability because atmospheric surface mixing tends to destroy shallow low-level temperature (Parish and Cassano, 2003).

Heat content. The seal-derived temperature measurements provided the first characterization of seasonal and interannual variability in upper ocean heat content in the innershelf region of the western Ross Sea. The total heat content includes all of the heat inputs and losses and as such provides a bulk measure of changes in the upper ocean temperature. The change in heat content from summer into winter for the three years shows the influence of synoptic scale events. The overall loss of heat expected from seasonal cooling is enhanced by strong wind events, such as the one early March 2010 for the Ross Island region and the one in late February-early March 2011 for the Victoria Land region. The persistence of heat in the upper water column into late March 2012 in both regions coincides with an extended period of weaker winds. The interannual variability in heat content may contribute to interannual variability in sea ice formation.

The evolution of the seal-derived heat content for the inner part of the Ross Sea can be compared to that calculated for the western Antarctic Peninsula (WAP), also based on temperature time series obtained from seal-derived measurements (Costa et al., 2008). The heat content for the innershelf regions of the Ross Sea is about 50% of the heat content along the WAP and reaches its minimum value about 2.5 months earlier. These differences are consistent with the higher latitude and the colder form of mCDW that occurs in the Ross Sea. The winter heat content of the Ross Sea is near zero; whereas that of WAP shelf waters remains around 50% of the late fall value. The implication is that the water column in the inner Ross Sea is essentially well mixed throughout the upper 300 m in winter as a result of convection. Winter mixing on the WAP shelf is shallower (Prézelin et al., 2004) and mixes warm mCDW (1-1.5^{o}C) into the upper water column (Klinck et al., 2004), thereby providing a continual source of heat. The quantitative comparisons of seasonal differences in heat content properties of the Ross Sea and WAP regions provided by the seal-collected measurements highlight the differences in cold (limited influence of CDW) versus warm (strongly influenced by CDW) Antarctic continental shelves.

Summary

In recent years, the Ross Sea has experienced changes in atmospheric conditions. Cold southerly winds blowing seaward from the Ross Sea Ice Shelf have strengthened, increasing vertical mixing (Turner et al., 2009; Smith et al., 2014b). However, projections of future winds over the Ross Sea suggest weakening relative to current conditions (Bracegirdle et al., 2013). A recent modeling study of the effects of these projected changes (Smith et al. 2014b) suggested that by 2100 winds near the coast will be weaker and stronger near the shelf break, mean summer mixed layer depths will decrease, and the duration of shallow mixed layers over the continental shelf will increase. The increased stratification implies a reduction in the vertical replenishment of surface nutrients with consequences for the continental shelf productivity (Smith et al. 2014a). Other potential changes by 2100 include a summer expansion of the Ross Sea polynya which will allow increased heat to the upper ocean from an extended time of solar radiation and also support an extended phytoplankton growing season (Smith et al., 2014b).

A reduction in wind strength over the next century will contribute to a more stratified coastal ocean. The results of this study show that the breakdown of summer stratification requires wind events with speeds above a particular threshold. Weakened winds may still have synoptic scale events that exceed this threshold, but the number and frequency of these is unknown. The simultaneous measurements of the ocean and atmosphere provide a means to continue to develop the understanding needed to evaluate future changes. Seal-derived hydrographic measurements are clearly adequate for providing the ocean state.

Expansion of the Ross Sea polynya will modify the inputs of less dense surface waters that form along the innershelf of the western Ross Sea Ice Shelf (Stern et al., 2014) and flow into the Ross Island region. Increased inputs of surface fresh water will contribute to enhanced stratification along the innershelf, requiring strong wind events to erode it.

The projected changes in the atmospheric conditions have important consequences for the thermohaline and sea ice properties of the coastal ocean along the innershelf of the western Ross Sea. These in turn will affect the Ross Sea food web (Smith et al., 2014b), but what changes may occur are essentially unknown (Piñones et al., 2015). The use of seals as platforms to measure and monitor the hydrography of the

Ross Sea will allow near synoptic views of environmental changes that can also be related to changes it seal ecology, behavior, and habitat use. The ability to measure evolving environmental and food web processes provides a strong constraint for implanting and evaluating circulation and ecological models designed to assess responses to projected changes in the Ross Sea.

Acknowledgments

This study was supported by the National Science Foundation Grants ANT-0944174 and ANT-0838911. A. Piñones also thanks FONDECYT/Chile 3150252 for support.

References

Årthun, M., K. W. Nicholls, K. Makinson, M. A. Fedak, Boehme, L., 2012. Seasonal inflow of warm water onto the southern Weddell Sea continental shelf, Antarctica. Geophysical Research Letters 39:L17601.

Bluhm, B.A., Coyle, K.O., Konara, B., Highsmith, R., 2007. High gray whale relative abundances associated with an oceanographic front in the south-central Chukchi Sea. Deep-Sea Research II 54: 2919-2933.

Bost, C. A., C. Cotté, F. Bailleul, Y. Cherel, J. B. Charrassin, C. Guinet, D. G. Ainley, and H. Weimerskirch. 2009. The importance of oceanographic fronts to marine birds and mammals of the southern oceans. Journal of Marine Systems 78:363-376.

Bost, C. A., C. Cotte, P. Terray, C. Barbraud, C. Bon, K. Delord, O. Gimenez, Y. Handrich, Y. Naito, C. Guinet, and H. Weimerskirch. 2015. Large-scale climatic anomalies affect marine predator foraging behaviour and demography. Nature communications 6:8220.

Bracegirdle, T.J., Stephenson, D.B., 2012. Higher precision estimates of regional polar warming by ensemble regression of climate model projections. Climate Dynamics 39: 2805–2821, doi:10.1007/s00382-012-1330-3

Bracegirdle, T.J., Shuckburgh, E., Salleé, J.-B., Wang, Z., Meijers, A.J.S., Bruneau, N., Phillips, T., Wilcox, L.J., 2013. Assessment of surface winds over the Atlantic, Indian, and Pacific Ocean sectors of the Southern Ocean in CMIP5 models: Historical bias, forcing response, and state dependence. Journal of Geophysical Research Atmosphere 118: 547–562, doi:10.1002/jgrd.50153.

Bromwich, D.H., 1991. Mesoscale cyclogenesis over the southwestern Ross Sea linked to strong katabatic winds. Monthly weather Review 119: 1736-1752

Budillon, G., Castagno, P., Aliani, S., Spezie, G., Padman, L., 2011. Thermohaline variability and Antarctic bottom water formation at the Ross Sea shelf break. Deep-Sea Research 58(10): 1002–1018, doi:10.1016/j.dsr.2011.07.002.

Burns, J.M., Costa, D.P., Fedak, M.A., Hindell, M.A., Bradshaw, C.J.A., Gales, N.J., McDonald, B., Trumble, S.J., Crocker, D.E., 2004. Winter habitat use and foraging behavior of crabeater seals along the Western Antarctic Peninsula. Deep-Sea Research II 51, 2279–230

Cassano, J. J., Parish, T. R., 2000. An analysis of nonhydrostatic dynamics in numerically simulated Antarctic katabatic flows. Journal of Atmospheric Science 57: 891–898.

Charrassin, J.-B., M. Hindell, S. R. Rintoul, F. Roquet, S. Sokolov, M. Biuw, D. Costa, L. Boehme, P. Lovell, R. Coleman, R. Timmermann, A. Meijers, M. Meredith, Y.-H. Park, F. Bailleul, M. Goebel, Y. Tremblay, C.-A. Bost, C. R. McMahon, I. C. Field, M. A. Fedak, and C. Guinet. 2008. Southern Ocean frontal structure and sea-ice formation rates revealed by elephant seals. Proceedings of the National Academy of Sciences 105:11634-11639.

Colacino, M., Piervitali, E., Grigioni, P., 2000. Climatic characterization of the Terra Nova Bay Region, in Ross Sea Ecology, edited by F.M. Faranda, L. Guglielmo and A. Ionora (Springer-Verlag, Berlin), 15-26

Comiso, J.C., Kwok, R., Martin, S., Gordon, A.L., 2011. Variability and trends in sea ice extent and ice production in the Ross Sea. Journal of Geophysical Research 116, C04021, doi:10.1029/2010JC006391.

Comiso, J.C. 2010. Polar Oceans From Space, 507 pp., Springer, New York.

Costa, D.P., Klinck, J.M., Hofmann, E.E., Dinniman, M.S., Burns, J.M., 2008. Upper ocean variability in west Antarctic Peninsula continental shelf waters as measured using instrumented seals. Deep-Sea Research II 55, 323–337.

Costa, D. P., G. A. Breed, Robinson, P.W., 2012. New Insights into Pelagic Migrations: Implications for Ecology and Conservation. Annual Review of Ecology, Evolution, and Systematics 43:73-96.

Dee, D. P., and 35 Coauthors, 2011. The ERA-Interim reanalysis: Configuration and performance of the data assimilation system. Quarterly Journal of the Royal Meteorological Society 137: 553–597, doi:10.1002/qj.828.

Dinniman, M.S., Klinck, J.M., Smith Jr., W.O., 2003. Cross-shelf exchange in a model of the Ross Sea circulation and biogeochemistry. Deep Sea Research II 50: 3103–3120

Dinniman, M.S., Klinck, J.M., Smith Jr., W.O., 2011. A model study of Circumpolar Deep Water on the west Antarctic Peninsula and Ross Sea continental shelves. Deep-Sea Research II 58: 1508–1523, doi:10.1016/j.dsr2. 2010.11.013.

Emery, W.J., Thomson, R.E., 1998. Data Analysis Methods in Physical Oceanography. Pergamon, New York, pp. 480e495.

Fedak, M. A., Lovell, P., Grant, S.M., 2001. Two approaches to compressing and interpreting time-depth information as collected by time-depth recorders and satellite-linked data recorders. Marine Mammal Science 17:94–110.

Fedak, M., Lovell, P., McConnell, B., Hunter, C., 2002. Overcoming constraints of long range radio telemetry from animals: getting more useful data from smaller packages. Integrative and Comparative Biology 42: 3–10.

Fedak, M. A. 2013. The impact of animal platforms on polar ocean observation. Deep Sea Research Part II: Topical Studies in Oceanography 88-89:7-13.

Gales, N.J., Mattlin, R.H., 1998. Fast, safe, field-portable gas anesthesia for otariids. Marine Mammal Science 14, 355–361

Goetz, K. T., 2015. Movement, habitat, and foraging behavior of Weddell seals (*Leptonychotes weddellii*) in the western Ross Sea, Antarctica. PhD Dissertation University of California Santa Cruz, p. 155.

Gordon, A.L., Orsi, A.H., Muench, R., Huber, B.A., Zambianchi, E., Visbeck, M., 2009. Western Ross Sea continental slope gravity currents. Deep-Sea Research II 56: 796-817

Gordon, A. L., B. A. Huber, Busecke, J., 2015. Bottom water export from the western Ross Sea, 2007 through 2010, Geophysical Research Letters 42: 5387–5394, doi:10.1002/2015GL064457.

Holland, P.R., Kwok, R., 2012. Wind-driven trends in Antarctic sea-ice drift. Nature Geoscience 5: 872-875

Imberger, J. 1985. The diurnal mixed layer. Limnology and Oceanography 30: 737–770.

Kaufman, D.E., Friedrichs, M.A.M., Smith Jr., W.O., Queste, B.Y., Heywood, K.J., 2014. Biogeochemical variability in the southern Ross Sea as observed by a glider deployment. Deep-Sea Research I 92: 93-106.

Klinck, J.M., Hofmann, E.E., Beardsley, R.C., Salihoglu, B., Howard, S., 2004. Water mass properties and circulation on the west Antarctic Peninsula continental shelf in austral fall and winter 2001. Deep-Sea Research II 51: 1925–1946.

Kohut, J., Hunter, E., Huber, B., 2013. Small-scale variability of the cross-shelf flow over the outer shelf of the Ross Sea. Journal of Geophysical Research Oceans 118: 1863-1876

Locarnini, R.A., 1994. Water masses and circulation in the Ross Gyre and environs. PhD Dissertation, Texas A&M University, p. 87.

Meredith, M. P., K. W. Nicholls, I. A. Renfrew, L. Boehme, M. Biuw, Fedak, M., 2011. Seasonal evolution of the upper-ocean adjacent to the South Orkney Islands, Southern Ocean: Results from a “lazy biological mooring”. Deep Sea Research Part II: Topical Studies in Oceanography 58:1569-1579.

Murphy, B.F., Simmonds, I., 1993. An analysis of strong wind events simulated in a GCM near Casey in the Antarctic. Monthly Weather Review 121: 522–534.

Orsi, A.H., Johnson, G.C., Bullister, J.L., 1999. Circulation, mixing, and production of Antarctic Bottom Water. Progress in Oceanography 43, 55–109.

Orsi, A.H., Wiederwohl, C.L., 2009. A recount of Ross Sea waters. Deep-Sea Research II 56: 778–795. doi:10.1016/j.dsr2.2008.10.033

Padman, L., D. P. Costa, S. T. Bolmer, M. E. Goebel, L. A. Huckstadt, A. Jenkins, B. I. McDonald, Shoosmith, D. R., 2010. Seals map bathymetry of the Antarctic continental shelf. Geophysical Research Letters 37:L21601.

Padman, L., D. P. Costa, M. S. Dinniman, H. A. Fricker, M. E. Goebel, L. A. Huckstadt, A. Humbert, I. Joughin, J. T. M. Lenaerts, S. R. M. Ligtenberg, T. Scambos, van den Broeke, M. R., 2012. Oceanic controls on the mass balance of Wilkins Ice Shelf, Antarctica. Journal of Geophysical Research 117: C01010, doi:10.1029/2011JC007301.

Parish, T.R., Bromwich, D.H., 1991. Continental-scale simulation of the Antarctic katabatic wind regime. Journal of Climate 4(2): 135–146.

Parish, T.R., Cassano, J.J., 2001. Forcing of the wintertime Antarctic boundary layer winds from the NCEP/NCAR global reanalysis. Journal of Applied Meteorology 40: 810–821.

Parish, T.R., Cassano, J.J., 2003. The role of katabatic winds on the Antarctic surface wind regime. Monthy Weather Review 131: 317–333

Parkinson, C.L., 2002. Trends in the length of the Southern Ocean sea-ice season. Annals of Glaciology, 34: 435–440,http://dx.doi.org/ 10.3189/172756402781817482.

Piñones, A., Hofmann, E.E., Dinniman, M.S., Davis, L.B., 2015. Modeling the transport and fate of euphausiids in the Ross Sea. Polar Biology DOI 10.1007/s00300-015-1798-5

Prézelin, B.B., Hofmann, E.E., Moline, M., Klinck, J.M., 2004. Physical forcing of phytoplankton community structure and primary production in continental shelf waters of the western Antarctic Peninsula. Journal of Marine Research 62, 419–460.

Roquet, F., Charrassin. J.-B., Marchand. S., Boehme, L., Fedak, M., Reverdin, G., Guinet, C., 2011. Delayed-mode calibration of hydrographic data obtained from animal-borne satellite relay data loggers. Journal of Atmospheric and Oceanic Technology 28: 787-801

Roquet, F., Y.-H. Park, C. Guinet, F. Bailleul, Charrassin, J.-B.. 2009. Observations of the Fawn Trough Current over the Kerguelen Plateau from instrumented elephant seals. Journal of Marine Systems 78:377-393.

Roquet, F., C. Wunsch, G. Forget, P. Heimbach, C. Guinet, G. Reverdin, J.-B. Charrassin, F. Bailleul, D. P. Costa, L. A. Huckstadt, K. T. Goetz, K. M. Kovacs, C. Lydersen, M. Biuw, O. A. Nøst, H. Bornemann, J. Ploetz, M. N. Bester, T. McIntyre, M. C. Muelbert, M. A. Hindell, C. R. McMahon, G. Williams, R. Harcourt, I. C. Field, L. Chafik, K. W. Nicholls, L. Boehme, Fedak, M. A. 2013. Estimates of the Southern

Ocean general circulation improved by animal-borne instruments. Geophysical Research Letters 40:6176-6180.

Rual, P., 1996. Onboard quality control of XBT bathy messages. Intergovernmental Oceanographic Commission of UNESCO and World Meteorological Organization Report IOC/INF-1021: Summary of ship-of-opportunity programmes and technical reports. Paris, 25 January 1996, 142–152.

Smith Jr., W.O., Asper, V., Tozzi, S., Liu, X., Stammerjohn, S.E., 2011. Surface layer variability in the Ross Sea, Antarctica as assessed by in situ fluorescence measurements. Progress in Oceanography 88: 28–45, http://dx.doi.org/10.1016/j.pocean.2010.08.002.

Smith Jr., W.O., Ainley, D.A., Arrigo, K.R., Dinniman, M.S., 2014b. The oceanography and ecology of the Ross Sea, Annual Review of Marine Science 6:
469–487, doi:10.1146/annurev-marine-010213-135114.

Smith Jr., W.O., M.S. Dinniman, E.E. Hoffman, and J. Klinck. 2014b. The effects of changing winds and temperatures on the oceanography of the Ross Sea in the 21st century. Geophysical Research Letters 41: 1624–1631, http://dx.doi.org/10.1002/2014GL059311.

Stammerjohn, S. E., Martinson, D.G., Smith, R.C., Yuan, X., Rind, D., 2008. Trends in Antarctic annual sea ice retreat and advance and their relation to ENSO and Southern Annular Mode variability. Journal of Geophysical Research 113, C03S90, doi:10.1029/2007JC004269.

Stammerjohn, S. E., Maksym, T., Heil, P., Massom, R. A., Vancoppenolle, M., Leonard, K. C., 2011. The influence of winds, sea-surface temperature and precipitation anomalies on Antarctic regional sea-ice conditions during IPY 2007, Deep Sea Research II 58: 999–1018, doi:10.1016/j.dsr2.2010.10.026.

Stern, A.A., Dinniman, M.S., Zagorodnov, V., Tyler, S.W., Holland, D.M., 2013. Intrusion of warm surface water beneath the McMurdo Ice Shelf Antarctica. Journal of Geophysical Research 118:7036–7048. doi:10. 1002/2013JC008842

Turner, J., Comiso, J.C., Marshall, G.J., Connolley, W.M., Lachlan-Cope, T.A., Bracegirdle, T., Wang, Z., Meredith, M., Maksym, T., 2009. Antarctic sea ice extent increases as a result of anthropogenic activity. Geophysical Research Letters 36, L08502, doi:10.1029/2009GL037524.

Figure Captions

Figure 1. (a) Map of Antarctica showing the location of the western Ross Sea (red box). The total number of CTD vertical profiles obtained from the tagged seals in 10 km^2 bins are shown for b) 2010, c) 2011, and d) 2012. Victoria Land (green box), Ross Island (blue box), and the mid-outer shelf (magenta box) were the regions with the largest number of seal-derived CTD profiles. Bathymetric contours are given in meters (color bar).

Figure 2. Salinity and potential temperature diagrams constructed from the seal-derived CTD measurements for summer (top panels) and fall-winter (lower panels) for the outer shelf (magenta), Victoria Land (green) and Ross Island (blue) regions for 2010, 2011 and 2012.

Figure 3. Time-depth distributions of density (top panels, kg m^{-3}) and buoyancy frequency (middle panels, s^{-2}) constructed using the seal-derived CTD measurements from the Ross Island region for a) 2010, b) 2011, and c) 2012. Time series of across-shore and alongshore wind speed (lower panels, m s^{-1}) were derived from the ERA-Interim reanalysis dataset.

Figure 4. Time-depth distributions of density (top panels, kg m^{-3}) and buoyancy frequency (middle panels, s^{-2}) constructed using the seal-derived CTD measurements from the Victoria Land region for a) 2010, b) 2011, and c) 2012. Time series of across-

shore and alongshore wind speed (lower panels, m s^{-1}) were derived from the ERA-Interim reanalysis dataset.

Figure 5. Lagged cross-correlation (in days) between across-shore wind (top panels), atmospheric pressure (middle panels) and atmospheric temperature (lower panels) and water density from 0 to 300 m for 2010, 2011 and 2012 in the Ross Island region. Positive (negative) correlations are indicated by warm (cool) colors.

Figure 6. Lagged cross-correlation (in days) between across-shore wind (top panels), atmospheric pressure (middle panels) and atmospheric temperature (lower panels) and water density from 0 to 300 m for 2010, 2011 and 2012 in the Victoria Land region. Positive (negative) correlations are indicated by warm (cool) colors.

Figure 7. Coherence (left panels) and phase (right panels) spectra calculated for across-shore wind and water density at five depths in the Ross Island region for 2010 (a, b), 2011 (c, d) and 2012 (e, f).

Figure 8. Coherence (left panels) and phase (right panels) spectra calculated for across-shore wind and water density at five depths in the Victoria Land region for 2010 (a, b), 2011 (c, d) and 2012 (e, f).

Figure 9. Wedderburn number estimated for (a) Ross Island and (b) Victoria Land for two mixed layer depths (MLD).

Figure 10. Total heat content calculated for the a) Ross Island and b) Victoria Land regions for 2010 (cyan), 2011 (black) and 2012 (red) from the seal-derived temperature data. Simulated sea ice fraction obtained from the Ross Sea circulation model described in Dinniman et al. (2011). The simulation provides sea ice for December 2010 to November 2012. Sea ice fraction for 2010-2011 (black) and 2011-2012 (red) is calculated from the area that is covered by sea ice.

Table Legends

Table 1. Summary of the CTD tags deployed on the Weddell seals in 2010, 2011 and 2012. The day of deployment, end of record and number of vertical profiles made by each instrumented seal is indicated.

Table 1

CTD tag indicator	Deployment (yyyy/mm/dd)	End record (yyyy/mm/dd)	Number of profiles
Ct63RS01	2010/02/04	2010/06/25	242
Ct63RS02	2010/01/27	2010/10/17	235
Ct63RS03	2010/01/27	2010/10/19	849
Ct63RS04	2010/01/29	2010/10/01	125
Ct63RS05	2010/01/29	2010/10/02	791
Ct63RS06	2010/01/25	2010/09/15	383
Ct63RS07	2010/01/25	2010/09/16	798
Ct63RS08	2010/01/29	2010/11/14	262
Ct63RS09	2010/01/29	2010/10/26	467
Ct63RS10	2010/01/29	2010/11/03	816
Ct63RS11	2010/02/02	2010/11/04	474
Ct63RS12	2010/02/01	2010/03/03	28
Ct63RS13	2010/02/01	2010/11/05	303
Ct63RS14	2010/02/01	2010/11/07	913
Ct63RS15	2010/02/02	2010/11/25	285
Ct63RS16	2010/02/03	2010/11/23	328
Ct63RS17	2010/02/03	2010/11/15	407
Ct63RS18	2010/02/03	2010/10/06	276
Ct63RS19	2010/02/04	2010/10/11	373
Ct63RS20	2010/02/05	2010/09/11	278
Ct63RS21	2010/02/09	2010/02/28	13
Ct63RS22	2010/02/08	2010/04/17	351
Ct63RS23	2010/01/30	2010/03/22	117
Ct63RS24	2010/02/05	2010/03/27	135
Ct63RS25	2010/02/08	2010/04/16	194
Ct63RS26	2010/02/08	2010/02/08	2
Ct63RS27	2010/02/04	2010/05/08	252
Ct74RS01	2011/01/29	2011/11/10	340
Ct74RS02	2011/01/29	2011/11/12	974
Ct74RS03	2011/01/28	2011/11/29	356
Ct74RS04	2011/02/07	2011/11/14	89
Ct74RS05	2011/01/27	2011/06/13	127
Ct74RS06	2011/01/28	2011/09/18	187
Ct74RS07	2011/02/25	2011/08/23	37
Ct74RS08	2011/02/05	2011/10/11	443
Ct74RS09	2011/02/05	2011/09/14	285
Ct74RS10	2011/02/03	2011/10/27	248
Ct74RS11	2011/01/30	2011/05/31	197
Ct74RS12	2011/02/05	2011/07/04	125
Ct74RS13	2011/01/27	2011/10/08	322
Ct74RS14	2011/01/27	2011/10/15	803

Ct74RS15	2011/01/31	2011/07/10	236
Ct74RS16	2011/01/29	2011/10/09	132
Ct74RS17	2011/02/09	2011/10/23	283
Ct74RS18	2011/02/09	2011/10/25	831
Ct74RS19	2011/01/22	2011/03/18	149
Ct74RS20	2011/02/10	2011/10/05	406
Ct74RS21	2011/02/03	2011/08/03	384
Ct74RS22	2011/01/31	2011/06/07	324
Ct88RS01	2012/02/06	2012/06/23	306
Ct88RS02	2012/01/28	2012/10/08	422
Ct88RS03	2012/02/01	2012/10/16	220
Ct88RS04	2012/01/27	2012/07/06	361
Ct88RS05	2012/01/28	2012/08/15	206
Ct88RS06	2012/01/24	2012/10/09	571
Ct88RS07	2012/01/29	2012/08/21	428
Ct88RS08	2012/02/01	2012/10/26	493
Ct88RS09	2012/02/02	2012/10/13	414
Ct88RS10	2012/01/25	2012/10/08	632
Ct88RS11	2012/01/27	2012/10/17	491
Ct88RS12	2012/02/03	2012/07/31	308
Ct88RS13	2012/01/29	2012/08/04	456
Ct88RS14	2012/01/30	2012/10/16	353
Ct88RS15	2012/02/03	2012/10/21	239
Ct88RS16	2012/01/31	2012/10/14	316
Ct88RS17	2012/02/10	2012/07/12	93
Ct88RS18	2012/02/08	2012/02/22	36
Ct88RS19	2012/02/08	2012/04/03	140

Figure(s)

Click here to download Figure(s): Figs_Seals_v28Jan2016.pdf

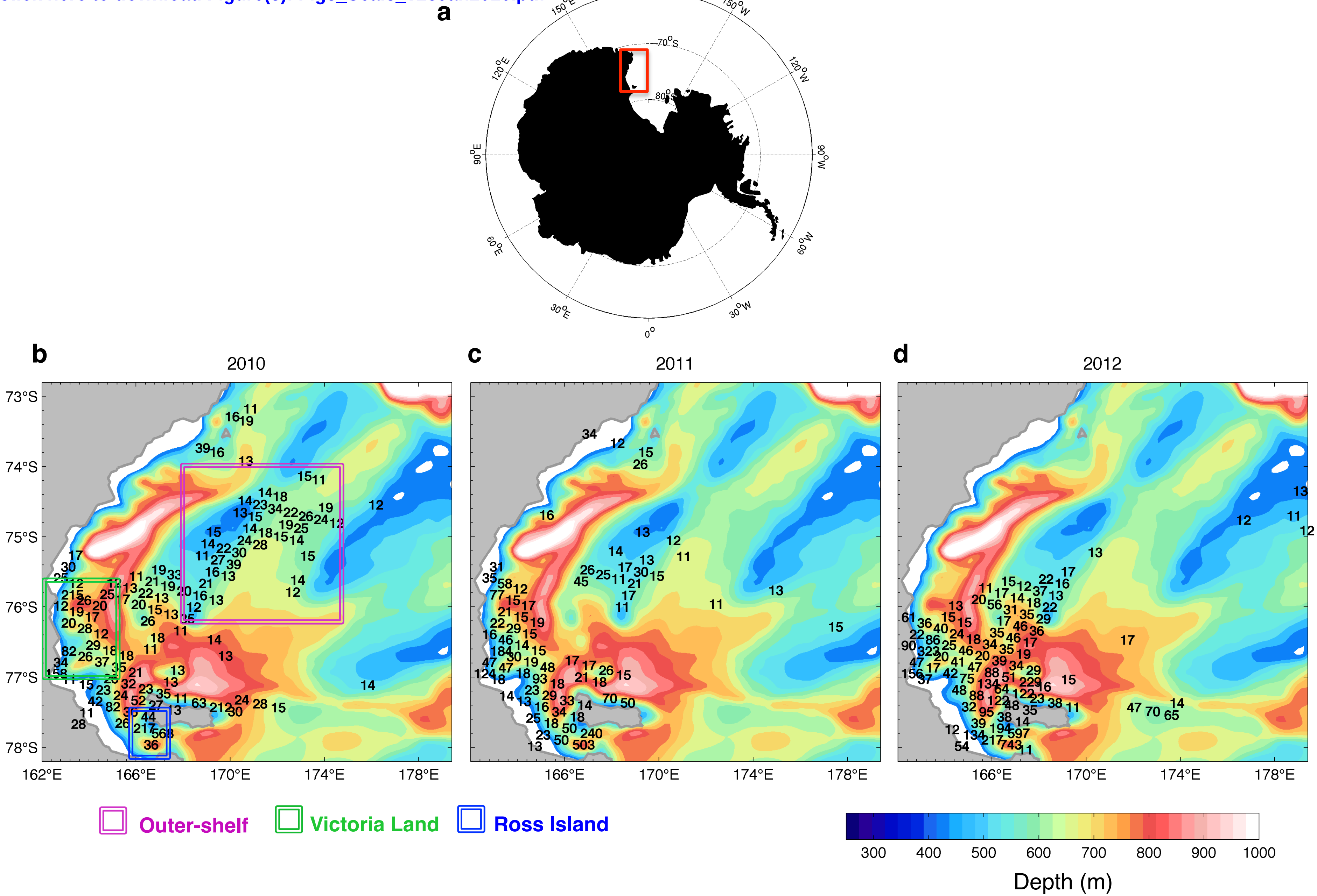

Figure 1

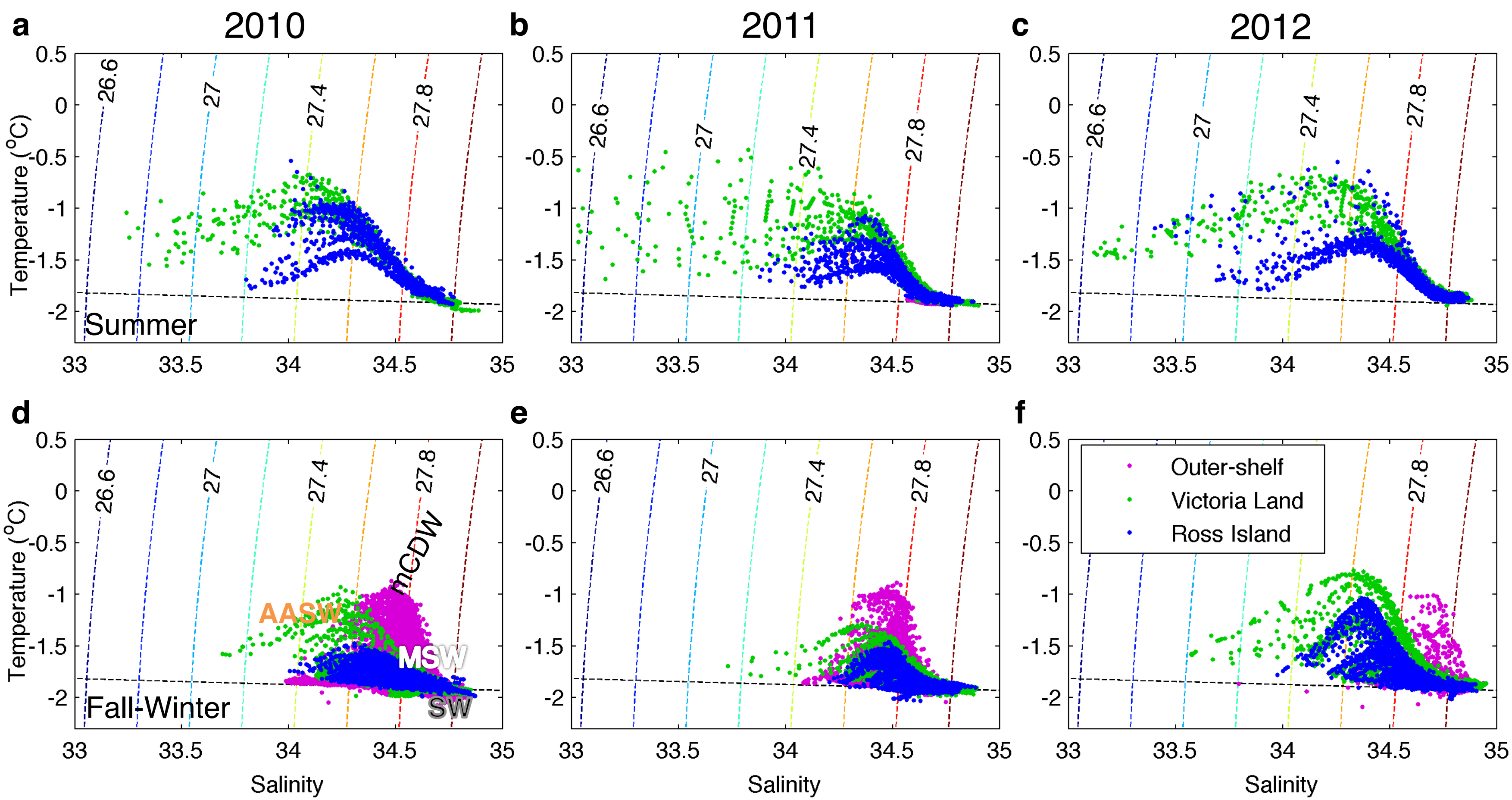
a
2010
b
2011
c
2012
Temperature (°C)
Summer
Salinity
d
e
f
AASW
mCDW
MSW
SW
Fall-Winter
Outer-shelf
Victoria Land
Ross Island
26.6
27
27.4
27.8

Figure 2

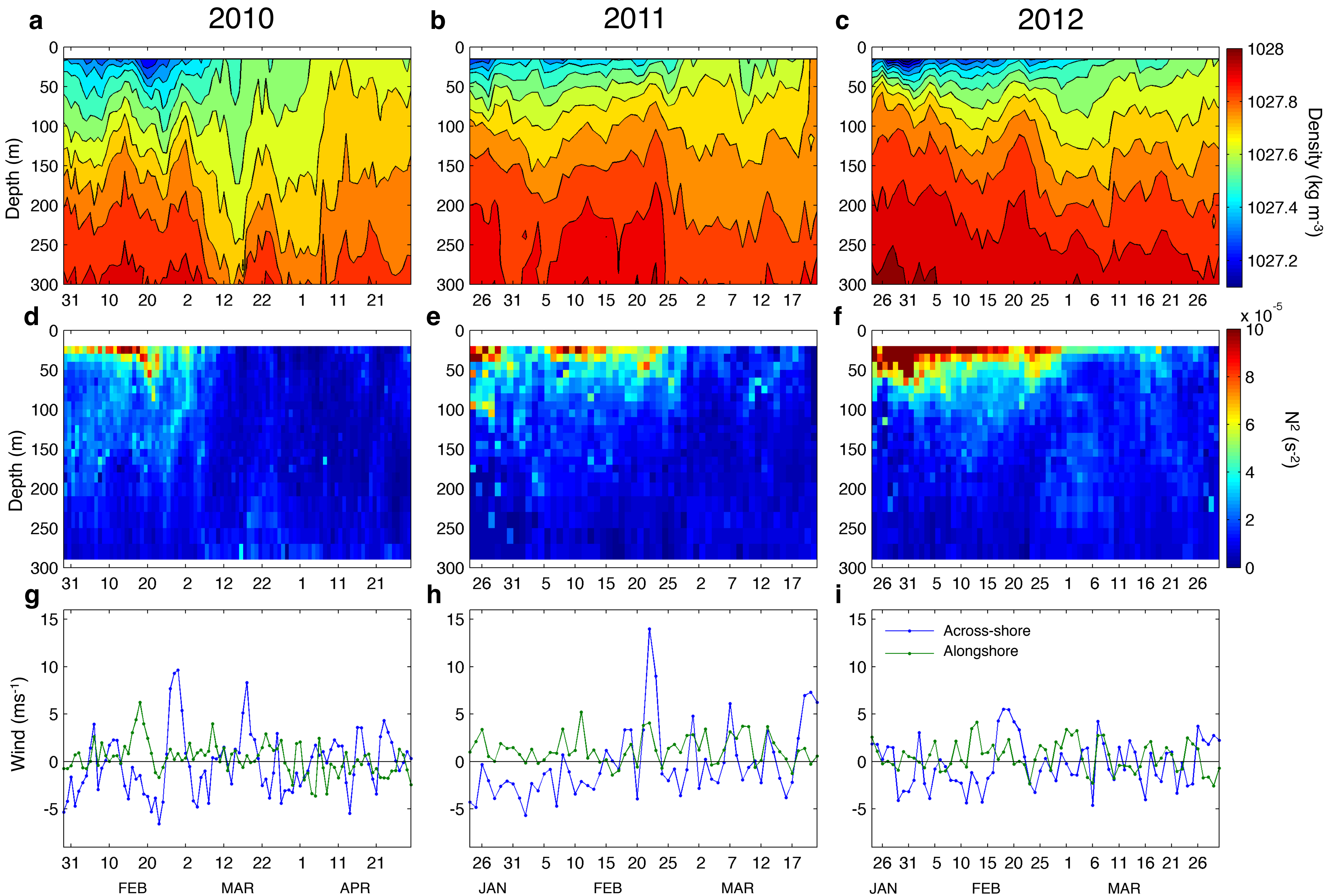

a
2010
b
2011
c
2012
Depth (m)
Density (kg m-3)
1028
1027.8
1027.6
1027.4
1027.2
d
e
f
x 10-5
N2 (s-2)
g
h
i
Wind (ms-1)
Across-shore
Alongshore
FEB
MAR
APR
JAN

Figure 3

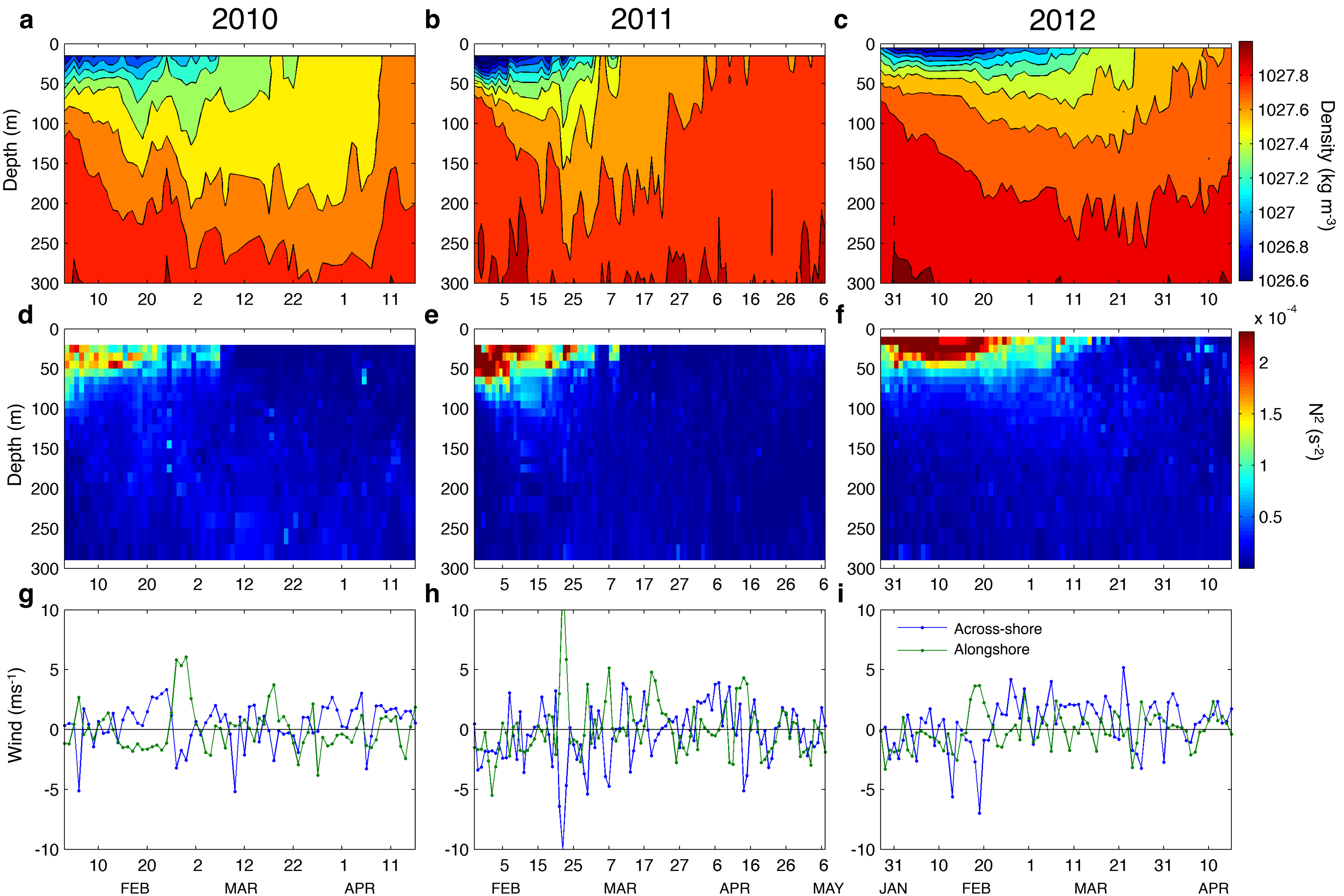

a
2010
b
2011
c
2012
Depth (m)
Density (kg m-3)
1027.8
1027.6
1027.4
1027.2
1027
1026.8
1026.6
d
e
f
x 10-4
N2 (s-2)
2
1.5
1
0.5
g
h
i
Wind (ms-1)
Across-shore
Alongshore
FEB
MAR
APR
MAY
JAN

Figure 4

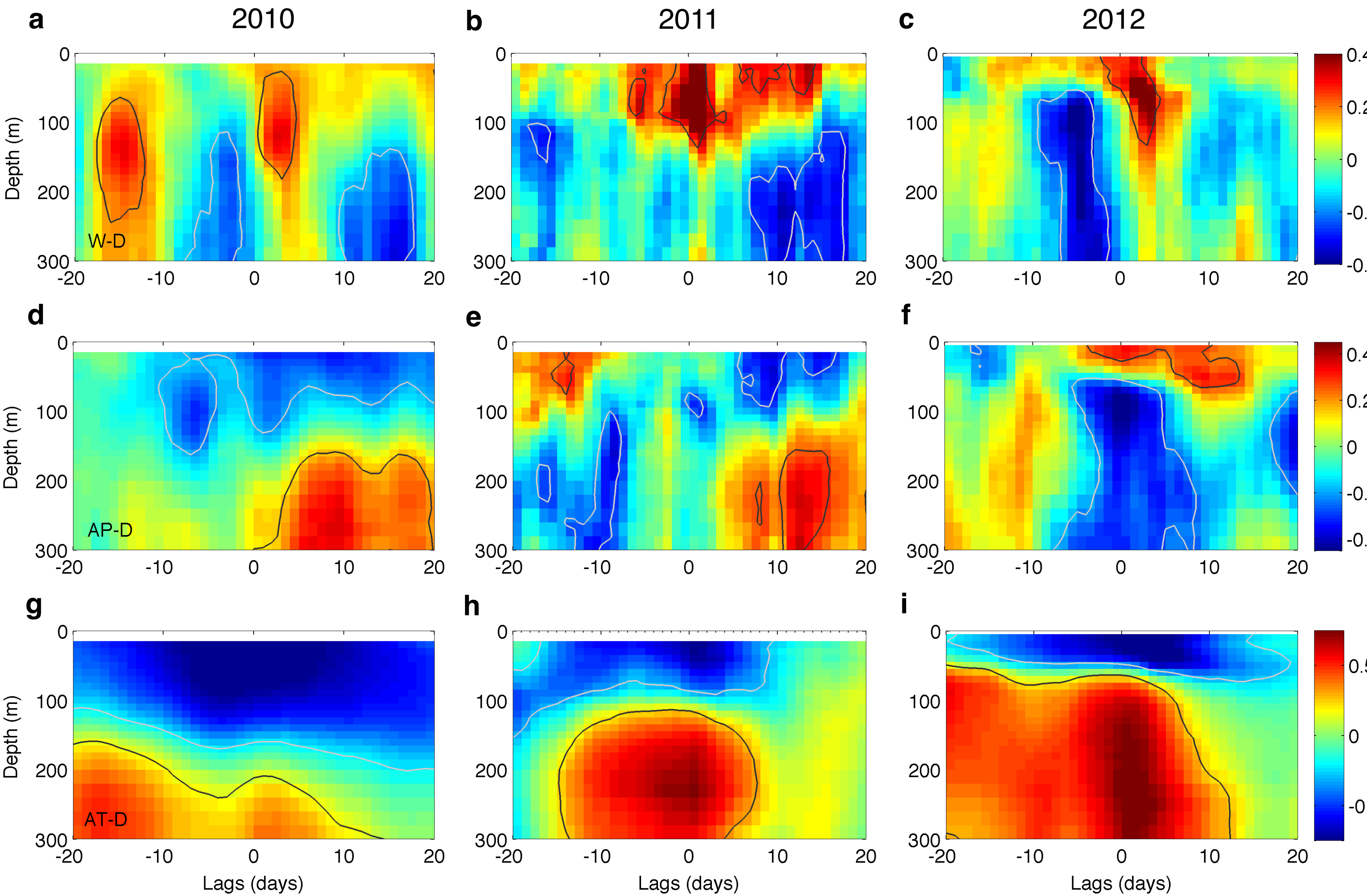

a
2010
b
2011
c
2012
d
e
f
g
h
i
Depth (m)
0
100
200
300
-20
-10
0
10
20
W-D
AP-D
AT-D
0.4
0.2
0
-0.2
-0.4
0.5
0
-0.5
Lags (days)

Figure 5

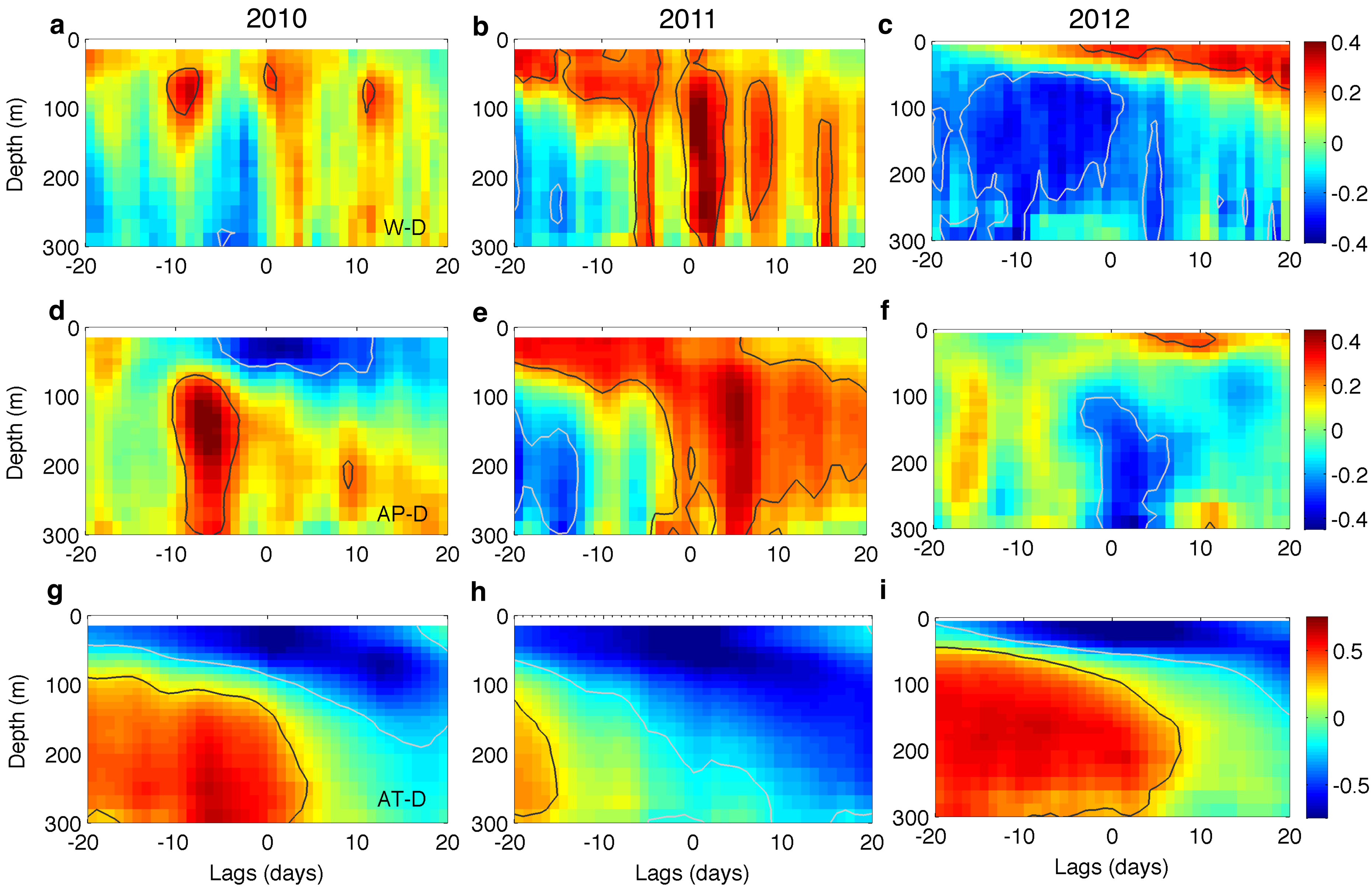

Figure 6

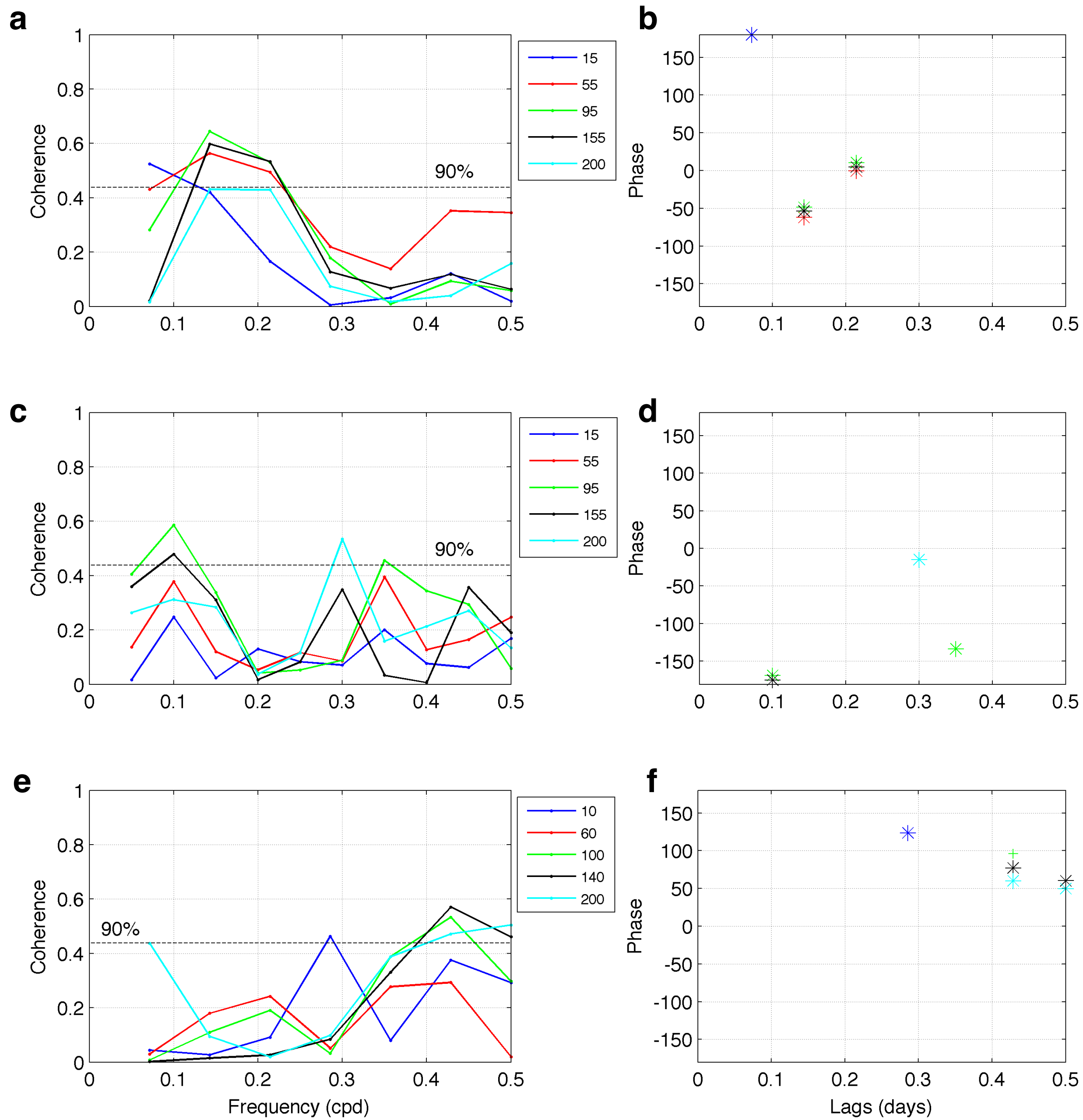

a
b
c
d
e
f
Coherence
Phase
90%
15
55
95
155
200
10
60
100
140
Frequency (cpd)
Lags (days)

Figure 7

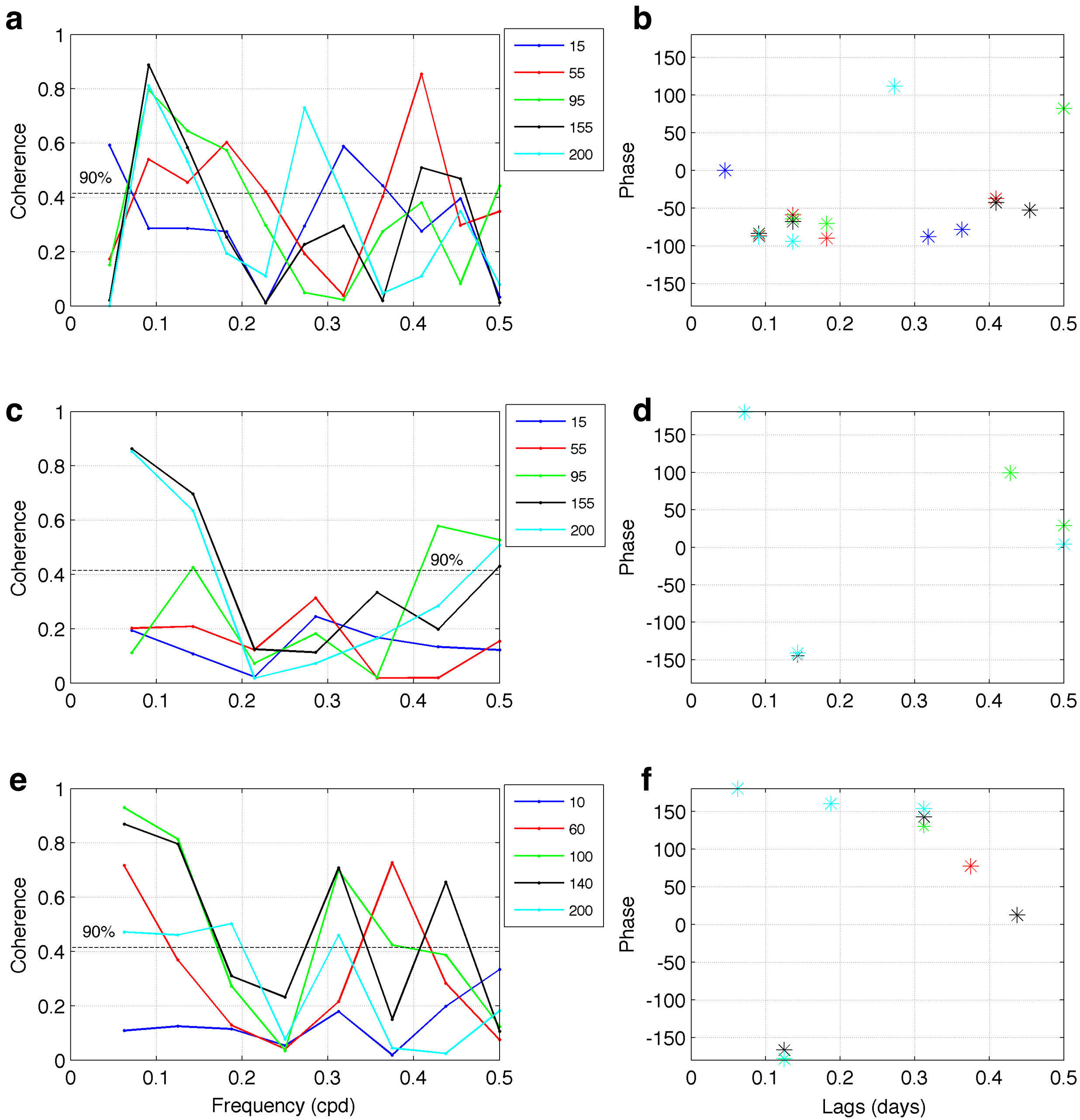
a
b
c
d
e
f
Coherence
Phase
Frequency (cpd)
Lags (days)
90%
15
55
95
155
200
10
60
100
140
200

Figure 8

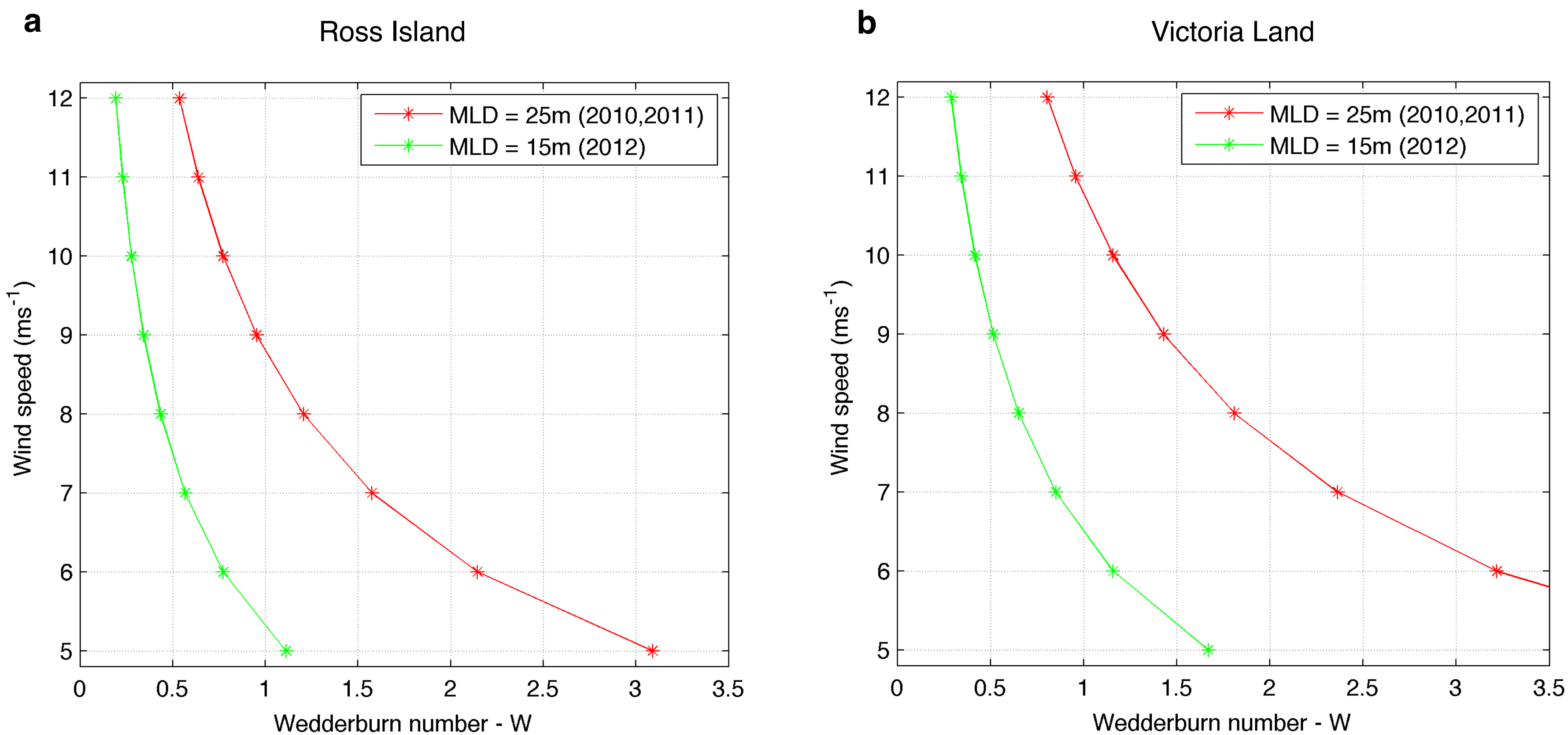

a
Ross Island
MLD = 25m (2010,2011)
MLD = 15m (2012)
Wind speed (ms^{-1})
Wedderburn number - W
b
Victoria Land
MLD = 25m (2010,2011)
MLD = 15m (2012)
Wind speed (ms^{-1})
Wedderburn number - W

Figure 9

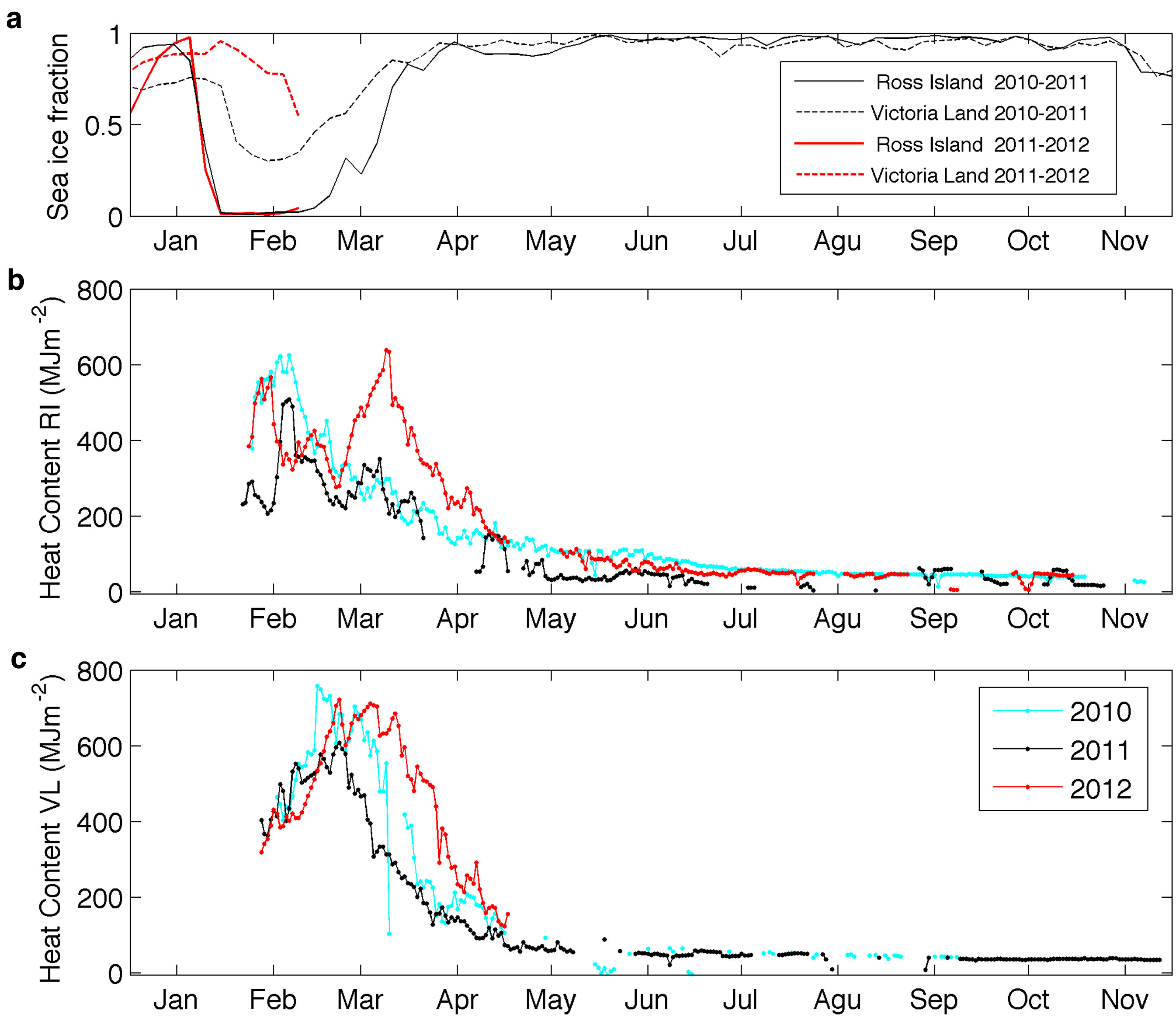

a
Sea ice fraction
1
0.5
0
Jan
Feb
Mar
Apr
May
Jun
Jul
Agu
Sep
Oct
Nov
Ross Island 2010-2011
Victoria Land 2010-2011
Ross Island 2011-2012
Victoria Land 2011-2012
b
Heat Content RI (MJm $^{-2}$)
800
600
400
200
0
c
Heat Content VL (MJm $^{-2}$)
2010
2011
2012

Figure 10